# CRISPR editing to mimic porphyria combined with light: A new preclinical approach for prostate cancer

Julian Boutin,[1,2] Coralie Genevois,[1,3] Franck Couillaud,[1,3] Isabelle Lamrissi-Garcia,[1] Veronique Guyonnet-Duperat,[1,4] Alice Bibeyran,[1,4] Magalie Lalanne,[1] Samuel Amintas,[1,5] Isabelle Moranvillier,[1] Emmanuel Richard,[1,2] Jean-Marc Blouin,[1,2] Sandrine Dabernat,[1,2] François Moreau-Gaudry,[1,2,6] and Aurélie Bedel[1,2,6]

[1]University of Bordeaux, INSERM, UMR 1312, Bordeaux Institute of Oncology, 146 Rue Léo Saignat, 33076 Bordeaux, France; [2]CHU de Bordeaux, Biochemistry Laboratory, 33000 Bordeaux, France; [3]Vivoptic Platform INSERM US 005—CNRS UAR 3427-TBM-Core, Bordeaux University, 33000 Bordeaux, France; [4]Vect'UB, Vectorology Platform, INSERM US 005—CNRS UAR 3427-TBM-Core, Bordeaux University, 33000 Bordeaux, France; [5]CHU de Bordeaux, Tumor Biology and Tumor Bank Laboratory, 33000 Bordeaux, France

**Thanks to its very high genome-editing efficiency, CRISPR-Cas9 technology could be a promising anticancer weapon. Clinical trials using CRISPR-Cas9 nuclease to *ex vivo* edit and alter immune cells are ongoing. However, to date, this strategy still has not been applied in clinical practice to directly target cancer cells. Targeting a canonical metabolic pathway essential to good functioning of cells without potential escape would represent an attractive strategy. We propose to mimic a genetic metabolic disorder in cancer cells to weaken cancer cells, independent of their genomic abnormalities. Mutations affecting the heme biosynthesis pathway are responsible for porphyria, and most of them are characterized by an accumulation of toxic photoreactive porphyrins. This study aimed to mimic porphyria by using CRISPR-Cas9 to inactivate *UROS*, leading to porphyrin accumulation in a prostate cancer model. Prostate cancer is the leading cancer in men and has a high mortality rate despite therapeutic progress, with a primary tumor accessible to light. By combining light with gene therapy, we obtained high efficiency *in vitro* and *in vivo*, with considerable improvement in the survival of mice. Finally, we achieved the preclinical proof-of-principle of performing cancer CRISPR gene therapy.**

## INTRODUCTION

The evolution of gene therapy is generating excitement in many disciplines. Early applications of gene therapy necessarily focused on relatively straightforward genetic disorders, such as severe combined immunodeficiency, whose aim was to replace the diseased gene by adding another gene *ex vivo* using retroviral/lentiviral vectors. Thereafter, innovative fundamental research and clinical practice led to the development of *in vivo* adeno-associated virus-based additive gene therapy for genetic disorders and the launch of innovative cancer gene therapies.[1] Either alone or in combination with conventional therapies, gene therapy possesses great potential to fight cancer; thus, cancer management quickly became the main target of gene therapy.[2] Most protocols involving *ex vivo* additive gene therapy do not directly target the cancer cells but rather the immune system. T lymphocytes are modified by a chimeric-antigen receptor (CAR) which helps the T cells bind to a specific cancer cell antigen in order to target the cancer cells.[3] Recently, CRISPR-Cas9 technology has revolutionized the gene therapy field. It enables precise insertions or deletions of specific DNA sequences at any point in the target DNA through the initiation of double-stranded breaks. In oncology, CRISPR-Cas9 has already been used to inactivate *PD1* or *TCR* in CAR-T cells *ex vivo* to boost their antitumor activity.[4] Another way to use CRISPR-Cas9 in cancer gene therapy could be to inactivate a key gene directly in a tumor. However, this promising approach is still underdeveloped.

In this context, canonical metabolic pathways are promising because they are highly conserved, even within a tumor, and are not dependent on tumor genomic heterogeneity/instability. Mimicking genetic metabolic disorders in cancer cells could be an alternative way to weaken them. Using expertise gained previously,[5–8] we propose to mimic porphyria by targeting the heme biosynthesis pathway, which is essential to the proper functioning of cells and without any possible escape. Heme biosynthesis pathway is a good candidate because (1) heme is a key compound in cancer cells[9] and (2) the blockade of heme biosynthesis results in the accumulation of photoreactive porphyrins and cell death after light exposure.[10] Thus, disruption of the heme biosynthesis pathway by CRISPR-Cas9 could generate an

abundant endogenous accumulation of intensely photoreactive porphyrins in cancer cells. Heme biosynthesis comprises eight enzymes whose deficiencies lead to genetic diseases.[11] In particular, congenital erythropoietic porphyria (CEP) is due to the deficiency of uroporphyrinogen synthase III (UROS), the fourth enzyme of heme biosynthesis, and induces the most severe skin lesions as a result of exposure to sunlight.[12] Therefore, *UROS* could be a target of choice to obtain photoreactive cancer cells. Moreover, unlike other heme enzyme deficiencies that could be directly lethal for cells and too risky, *UROS* inactivation does not impair cell viability without light exposure—in other words, patients with CEP only have light-induced skin and hematological lesions. *UROS* inactivation could serve as a prodrug in a two-step approach by combining CRISPR editing and tumor illumination. Importantly, gene therapy associated with light exposure offers the opportunity for safe focal treatment with high specificity in illuminated cancer cells.

The model for this proof-of-concept is prostate cancer. It is the second most frequent cancer and the fifth most common cause of cancer mortality in men.[13] It is a good candidate thanks to its anatomical site, which enables direct intraprostatic injections that facilitate *in situ* gene therapy protocols and the application of light. The first *in situ* gene therapy clinical trial in prostate cancer started in 1999, and a wide range of gene therapy concepts have been developed since then.[14] Here, we propose an innovative strategy and demonstrate that the inactivation of the *UROS* gene by CRISPR-Cas9-nuclease induces the high accumulation of photoreactive porphyrins in cancer cells, leading to antitumor efficacy both *in vitro* and *in vivo*. It leads to a metabolic tumor vulnerability. It opens an avenue for cancer gene therapy by targeting a canonical pathway and mimicking metabolic disorders to weaken cancer cells, independent of their genomic abnormalities.

## RESULTS

### CRISPR-Cas9-mediated *UROS* inactivation sensitizes prostate cancer PC3 cells to 405-nm light *in vitro*

The first step was to inactivate *UROS* to induce photoreactive red fluorescent type I porphyrin accumulation in cells (Figure S1A). We designed a lentiviral vector containing the CRISPR-Cas9 nuclease sequence, a guide RNA (gRNA) against *UROS* and a Zs-Green reporter sequence to visualize transduction efficiency by flow cytometry (Figure 1A). We efficiently transduced the human prostate cancer cell line (PC3) expressing prostate-specific membrane antigen (PSMA) (PC3-PIP), with up to 95% of cells expressing Zs-Green detected by cytometry (*UROS* knockout [KO] PC3 cells; Figure 1B). Transduction of this vector induced a high rate of insertions/deletions (indels) (>90%) in the targeted *UROS* (Figure S1B). UROS activity deficiency is known to induce metabolic heme biosynthesis dead-end with endogenous fluorescent porphyrin accumulation (detectable in Per-CP [peridinin chlorophyll protein complex] cytometry channel). To validate metabolic UROS deficiency, we monitored the kinetic of the fluorescent Per-CP$^+$ cells appearance. Fourteen days after *UROS* gene editing, we achieved >90% Per-CP$^+$ cells by cytometry (Figure 1B, left and center panels), proof of the *UROS* inactivation. We

also confirmed the high porphyrin accumulation in cells by spectrofluorimetry (Figure 1B, right panel). Porphyrin detection was stable over time (i.e., at least 26 days). These data validated the CRISPR approach to edit *UROS* and to induce the endogenous accumulation of porphyrins. To test the photosensitivity of PC3 cells after *UROS* editing, we performed illumination at 405 nm, the major type I porphyrin absorbance wavelength (Soret band). We carried out a scale-dose of light from 2 to 20 J/cm$^2$ in wild-type (WT) and *UROS* KO PC3 cells to evaluate the cell death induced. From 2.5 J/cm$^2$ (corresponding to 1 min of light), light induced the cell death of *UROS* KO PC3 cells (higher than 95%, p < 0.001 compared to WT cells with light). Importantly, all of the *UROS* KO PC3 cells died with 20 J/cm$^2$, without any toxicity in WT PC3 cells (Figure 1C). Together, these data demonstrate the efficiency of *UROS* inactivation coupled with a 405-nm light exposure to induce the death of prostate cancer cells.

### *UROS* inactivation sensitizes prostate cancer PC3 cells to 405-nm light *in vivo* but induces dermatoxicity

We next decided to confirm our *in vitro* results in an *in vivo* three-dimensional model. To monitor tumor growth, we modified human PC3 cells (WT and *UROS* KO) to express luciferase to obtain a noninvasive and sensitive bioluminescence-based tumor quantification method. We subcutaneously xenografted PC3 cells on the two contralateral flanks of immunodeficient NSG mice to obtain either two tumors with WT PC3 cells (blue) or two tumors with *UROS* KO PC3 cells (red) per mouse. After 7 days, we illuminated only one tumor of each mouse with a single dose of 405-nm light (20 J/cm$^2$, corresponding to 8 min). To measure the illumination efficacy, we measured the bioluminescence of tumors for 4 days after treatment and weighed the tumors at sacrifice at day 4 (Figure 2A). Whereas illumination did not modify the tumor growth in WT PC3 tumors (blue), 405-nm light drastically reduced bioluminescence intensity in *UROS* KO PC3 tumors (red) (Figures 2B and 2C). The weight of tumors at sacrifice 4 days after illumination confirmed the specific effect of 405-nm light on *UROS* KO PC3 tumors (Figure 2D). With only one dose of 405-nm light, *UROS* KO PC3 tumors were one-third of the weight of nonilluminated *UROS* KO PC3 control tumors. No significant effect of lighting was observed in WT PC3 tumors. These *in vivo* data demonstrated the antitumor efficiency of 405-nm light exposure on UROS-deficient cancer cells in subcutaneous prostatic tumors. Unfortunately, extensive dermatoxicity with skin burns and damage to the areas illuminated with 405-nm light was observed in all of the mice, regardless of UROS functionality (Figure 2E).

### Alternative wavelengths for *in vitro* illumination of *UROS*-inactivated PC3 cells

To reduce dermatoxicity and increase light penetrance while maintaining the efficacy of gene therapy, we applied longer light wavelengths at Q-band porphyrin absorption. We tested 530-nm and 660-nm wavelengths (Figure 3A). With 530 nm, we obtained a scale-dose effect on *UROS* KO PC3 cells, with a partial effect from 24 J/cm$^2$ (half-maximal inhibitory concentration) and a drastic reduction in cell count at 120 J/cm$^2$ (corresponding to 20 min)
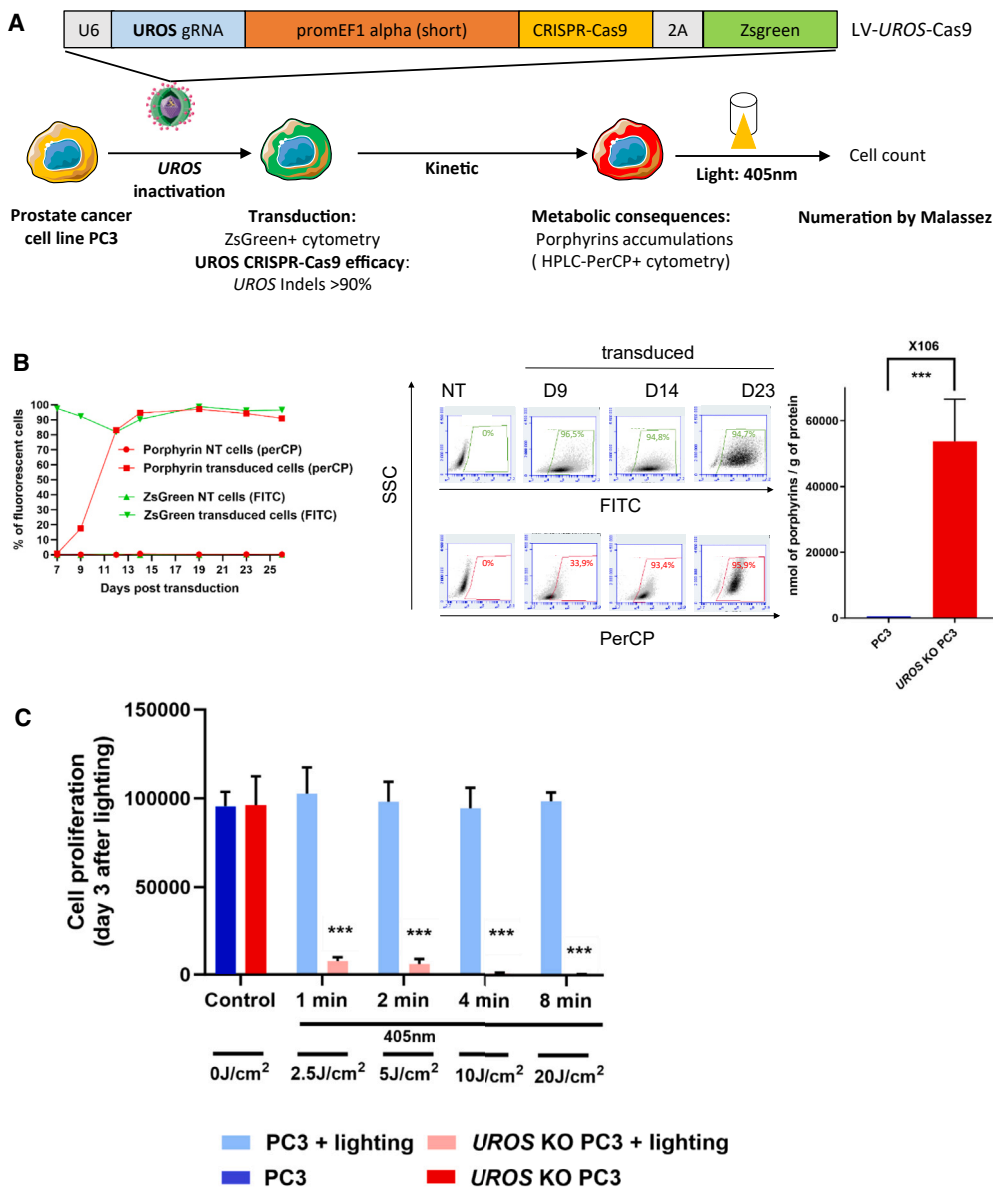
**Figure 1. CRISPR-Cas9-mediated *UROS* inactivation induces *in vitro* human prostate cancer PC3 cell death after a single 405-nm illumination session**

(A) Top: LV-*UROS*-Cas9 lentiviral vector schema used for *UROS* inactivation by CRISPR-Cas9. The LV-*UROS*-Cas9 vector contains the U6 promoter (pU6) for *UROS* gRNA, EF1-α promoter (pEF1-α) drives CRISPR-Cas9 nuclease expression, followed by a 2A self-cleaving peptide and a Zs-Green reporter gene to monitor transduction. Bottom: Experimental design. After transduction of PC3 human prostate cancer cells by LV-*UROS*-Cas9, *UROS* inactivation is checked by *UROS* gene sequence analysis and by porphyrin accumulation assay (cytometry and HPLC). Efficacy of the approach is tested by a scale-dose of light at 405 nm. (B) Left and center: Kinetics and representative dot plots of transduction efficacy (Zs-Green/FITC⁺) and *UROS* inactivation (fluorescent porphyrin appearance, PerCP⁺) after LV-*UROS*-Cas9 transduction in PC3 cells by cytometry. Right: Porphyrin quantification by HPLC in transduced (*UROS* KO, red) or nontransduced PC3 cells (blue). Mean ± SD, n = 4. (C) Scale-dose of 405-nm light (from 2.5 to 20 J/cm²) on *UROS* KO (red) and nontransduced (blue) PC3 cells. Cell count 3 days after illumination. Mean ± SD, n = 8. Statistical differences were determined by Mann-Whitney post-Kruskal-Wallis test. \*\*\*p < 0.001.

(p < 0.01). In contrast, illumination did not modify the cell count of WT PC3 cells (Figure 3B). The 660-nm wavelength induced only a partial reduction of the *UROS* KO PC3 cell count, even at the highest dose (230 J/cm², Figure 3C). We thus used 530-nm light exposure thereafter as a compromise between penetrance and efficiency.

Because *in vivo* gene therapy cannot target all of the tumor cells, a bystander effect would assist tumor regression. To evaluate the bystander effect of our strategy, we mixed 25% of *UROS* KO PC3 cells with 75% of WT PC3 cells *in vitro and* quantified the proportion of fluorescent cells 3 days after a single dose of 530-nm light exposure
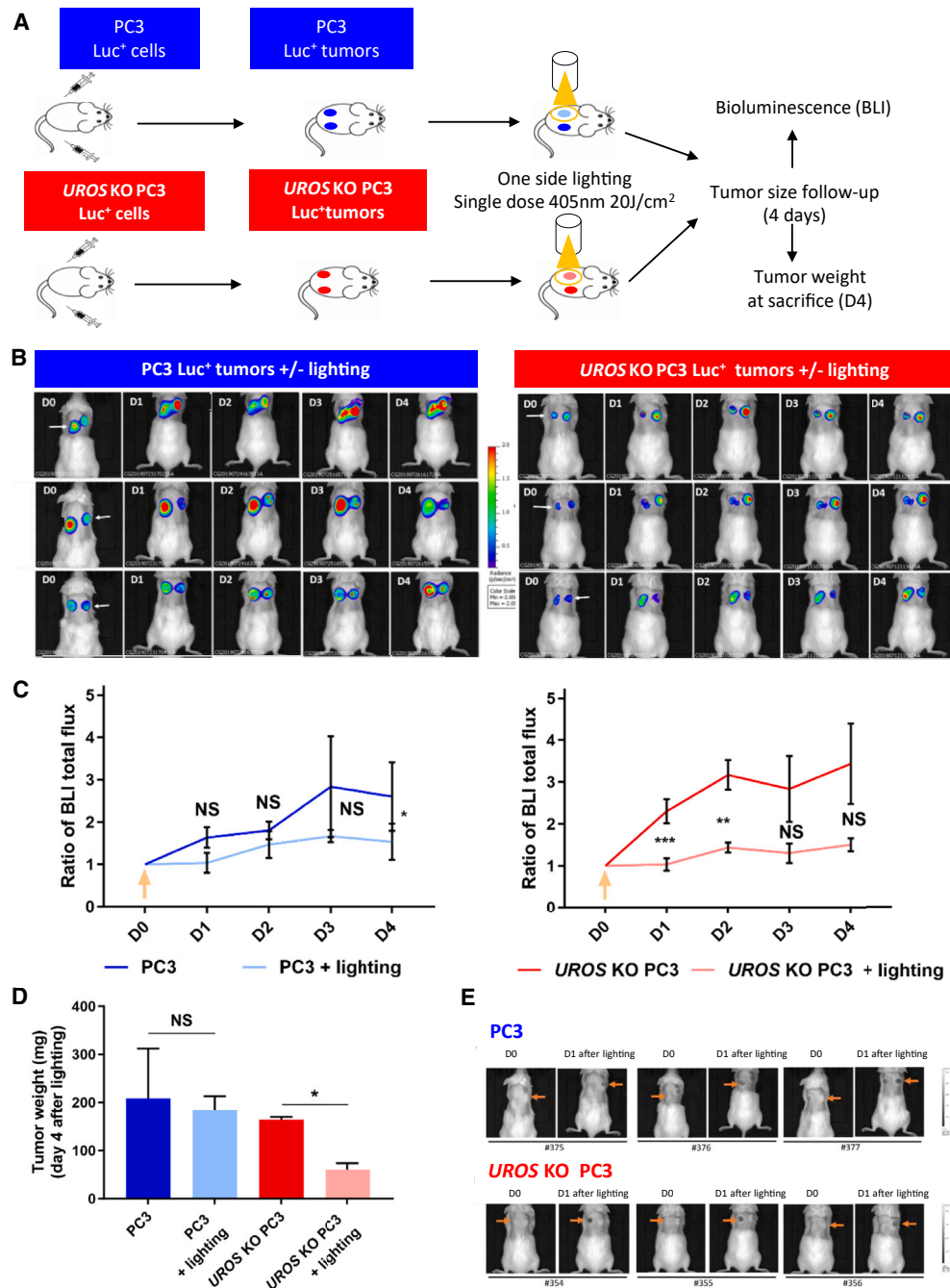
**Figure 2. Tumor regression with LV-*UROS*-Cas9 combined with 405-nm lighting is associated with dermatoxicity**

(A) Experimental design. PC3 cells were first transduced with an LV-containing luciferase gene (Luc[+] PC3) for *in vivo* tumor BLI monitoring. Then, Luc^{+} PC3 cells were transduced or not with LV-*UROS*-Cas9 to inactivate *UROS* or not. Immunodeficient (NSG) mice were injected (subcutaneously) in both contralateral flanks with either Luc[+] PC3 (blue) or *UROS* KO Luc[+]PC3 (red). After 7 to 10 days, one side of the tumor of each mouse was irradiated by a single dose of 405-nm light for 8 min (20 J/cm^{2}). Tumor size was measured each day by BLI monitoring and tumor weight 4 days after illumination. n = 3 mice per group. (B) Bioimaging of tumor over time. Left: Luc[+] PC3 tumors (blue), and right: with *UROS* KO Luc[+] PC3 tumors (red). Each irradiated tumor is indicated by a white arrow. (C) Kinetic of tumor BLI quantification after lighting. Results are expressed by the ratio of total BLI flux considering 1 as the day of illumination. Mean ± SEM. Statistical differences were determined by paired t test post-Shapiro test for normality or nonparametric Wilcoxon when the Shapiro test failed. ns, *p < 0.05. (D) Weight of tumors after sacrifice 4 days after illumination. Mean ± SEM, 3 tumors per group. Statistical differences were determined by paired t test post-Shapiro test for normality. ns, not significant; *p < 0.05. (E) Photographs of dermatoxicity 1 day after a 405-nm single dose of light. Orange arrows indicate irradiated tumors.
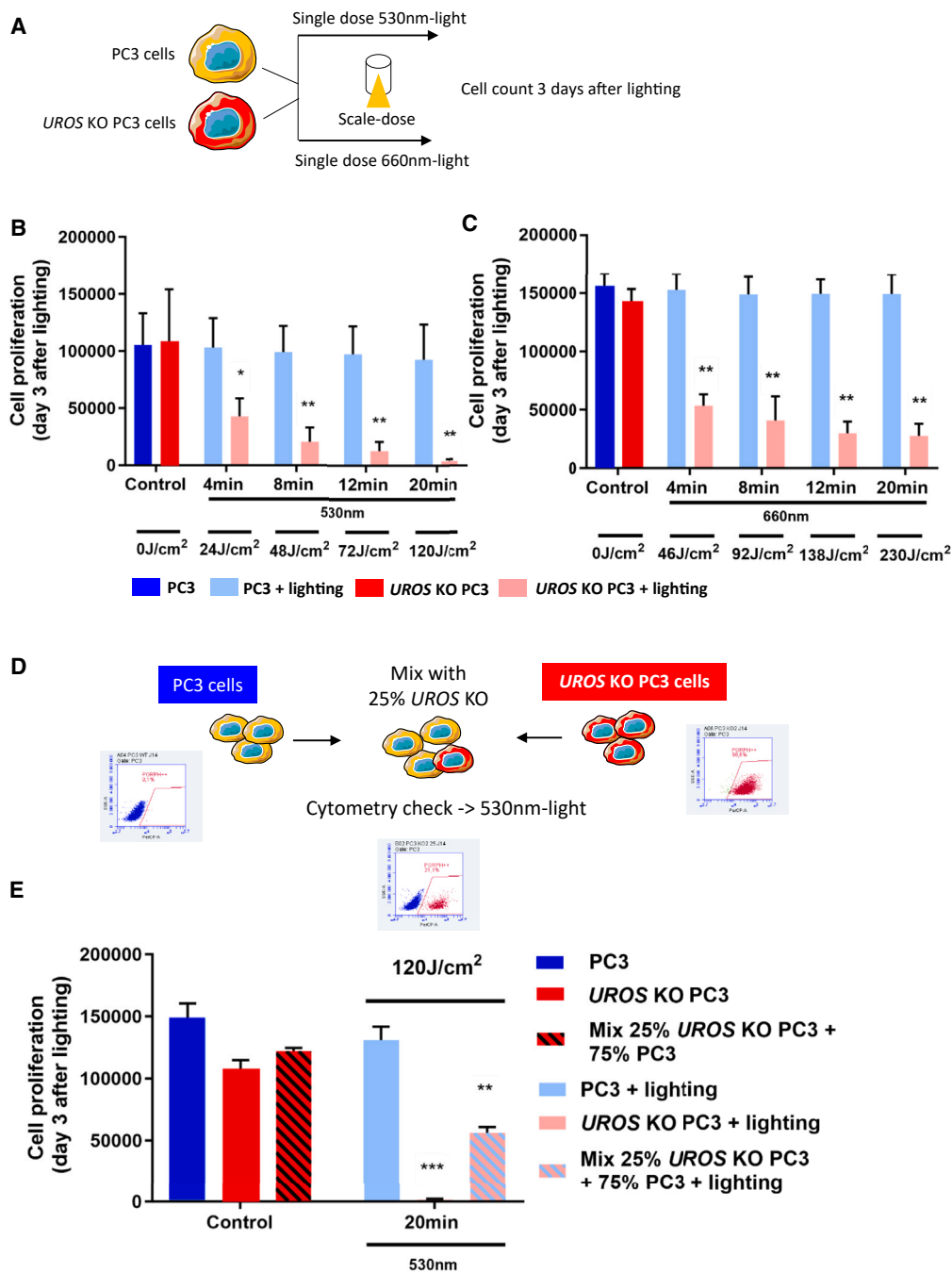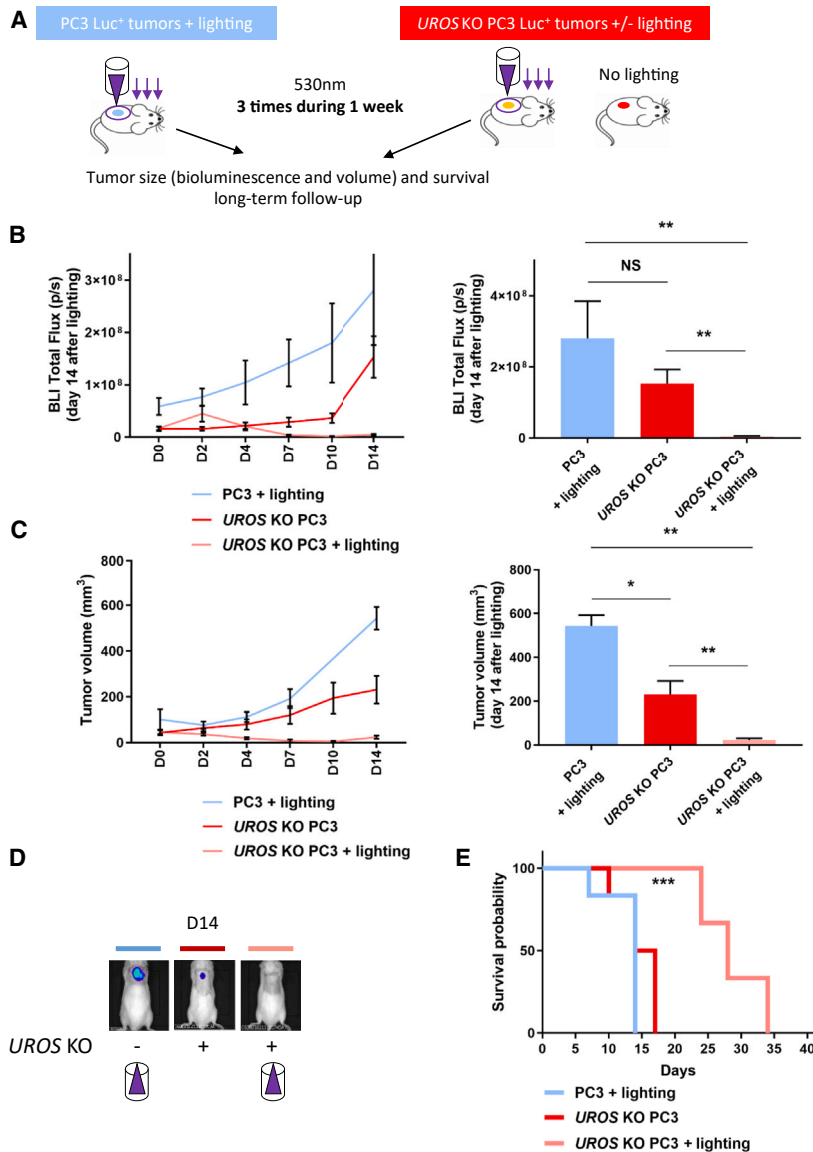
**Figure 3. *In vitro* evaluation of alternative porphyrin excitation wavelength efficiencies**

(A) Experimental design. Scale-dose of a single dose of light at 530 nm (B) (from 24 to 120 J/cm$^2$) or 660 nm (C) (from 46 to 230 J/cm$^2$) on PC3 cells, inactivated or not for *UROS*. Cell count 3 days after lighting. PC3 cells in blue. Dark blue, without light. Light blue, with lighting. *UROS* KO PC3 cells in red. Dark red, without light. Pink, with lighting. Mean ± SD, n = 6. Statistical differences were determined by Mann-Whitney post-Kruskal-Wallis test. *p < 0.05, **p < 0.01. (D) Experimental design. Mix of Luc+ PC3 (blue, 75%) and *UROS* KO Luc+ PC3 (red, 25%) cells. Proportion was checked by cytometry. *UROS* KO Luc+ PC3 are PerCP-fluorescent due to porphyrin accumulation, before *in vitro* and *in vivo* evaluation of treatment efficacy to eliminate cells. (E) *In vitro* effect of a single dose (120 J/cm$^2$, 20 min) of 530-nm light, mean ± SD, n = 6. Cell count 3 days after lighting. Mix is represented by hatched column. Statistical differences were determined by Mann-Whitney post-Kruskal-Wallis test, comparing before and after illumination. **p < 0.01, ***p < 0.001.

**Figure 4. *UROS* inactivation combined with repeated 530-nm light induces PC3 tumor regression *in vivo***

(A) Experimental design. Luc⁺ PC3 (blue) and *UROS* KO Luc⁺ PC3 (red) cells were subcutaneously injected in NSG mice (1 side), and irradiated (or not) 3 times per week (D0, Monday; D2, Wednesday; D4, Friday) for 1 week at 530 nm. Illumination is indicated by the purple light. Six mice per group. Follow-up of BLI, tumor volume, and mice survival for 17 days (sacrifice). (B) Monitoring of tumor growth by BLI quantification over time (left) and at day 14 (right). Mean ± SEM. Statistical differences were determined by Mann-Whitney post-Kruskal-Wallis test. NS, not significant, **p < 0.01. (C) Volume of tumor growth over time (left) or at day 14 (right). Crosses mean that all of the mice in a group are dead. Mean ± SEM. Statistical differences were determined by Mann-Whitney post-Kruskal-Wallis test. NS, not significant, *p < 0.05, **p < 0.01. (D) Absence of dermatoxicity with repeated 530-nm illumination. (E) Kaplan-Meier plot for survival of mice with PC3 tumors treated or not by LV-*UROS*-Cas9 and repeated 530-nm light. Statistical difference by Mantel-Cox test.

tumor volumes by caliper. As observed in Figure 2B with BLI, *UROS* KO PC3 tumors were slightly smaller at the beginning of the experiment (BLI assay and volume measurement at day 0; Figures 4B and 4C, left panels), probably due to light exposure during injection. Repeated 530-nm light for 1 week dramatically reduced tumor BLI signal intensities and tumor volumes. Tumors were undetectable at days 7–10, even by BLI. At day 14, BLI intensities and volumes of illuminated *UROS* KO PC3 tumors were, respectively, 32- and 10-fold lower than those of nonilluminated *UROS* KO PC3 tumors (Figures 4B and 4C, right panels, and illustrative Figure 4D). Moreover, no dermatoxicity was observed with repeated 530-nm light exposure for 1 week (Figure 4D). Importantly, gene therapy associated with iterative 530-nm light for 1 week doubled the survival of mice (34 days versus 17 days with *UROS* KO PC3 tumors) (Figure 4E).

(Figure 3D). A 50% drop in cell count was observed (i.e., 2-fold greater than the initial proportion of porphyrin cells), thus confirming the presence of a bystander effect (p = 0.0022) (Figure 3E).

### *UROS* inactivation combined with repeated 530-nm light induces PC3 tumor regression *in vivo*

To evaluate the efficiency of *UROS* gene therapy combined with 530-nm light *in vivo*, we subcutaneously grafted either WT or *UROS* KO PC3 cells in NSG mice to obtain one PC3 tumor per mouse. We next performed repeated 530-nm illuminations (i.e., 3 times per week, days 0, 2, and 4) on PC3 WT and *UROS* KO PC3 tumors (Figure 4A). One control group of nonilluminated *UROS* KO PC3 tumors was also included in the experiment. We monitored tumor bioluminescence imaging (BLI) (Figure S2) and

### *UROS* inactivation in PC3 cells combined with long-term repeated 530-nm light increases mice survival

Because we observed a slight relapse at ∼day 17 after three 530-nm illumination sessions, we tried to extend the remission period by maintaining the same illumination protocol for 5 weeks (Figure 5A). Again, 530-nm light was very efficient in blocking *UROS* KO PC3 tumor progression during the first 2 weeks (Figure 5B). Unfortunately, it did not avoid a secondary tumor relapse during week 3. To understand whether tumor relapses were due to (1) the persistence and selection of *UROS* WT cells that are not light sensitive or (2) a reduction in the efficiency of light after 2 weeks, we assessed the *UROS*
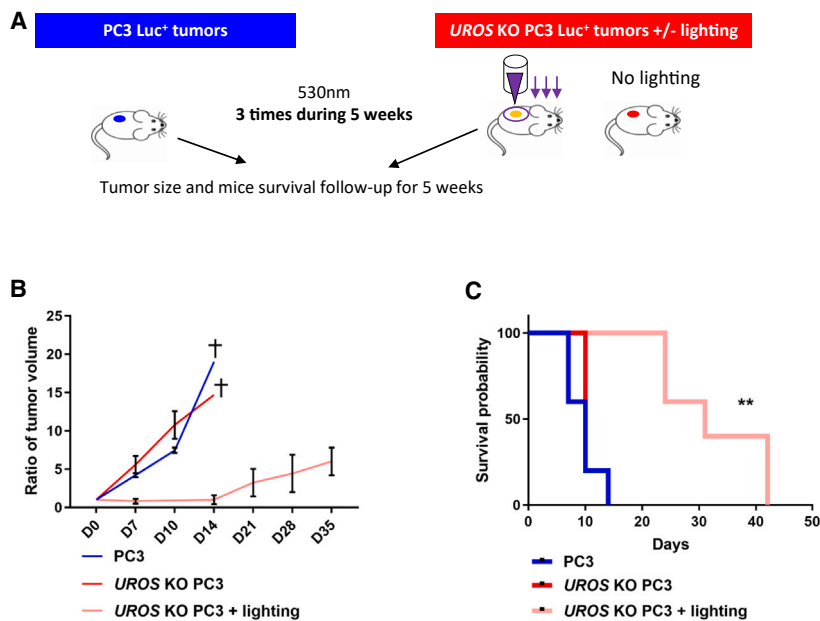
**A**

PC3 Luc⁺ tumors

*UROS* KO PC3 Luc⁺ tumors +/- lighting

530nm
**3 times during 5 weeks**

No lighting

Tumor size and mice survival follow-up for 5 weeks

**B**

**C**

PC3
*UROS* KO PC3
*UROS* KO PC3 + lighting

**Figure 5. *UROS* inactivation in PC3 cells combined with long-term repeated 530-nm light increases mice survival**

(A) Experimental design. Luc⁺ PC3 (blue) and *UROS* KO Luc⁺ PC3 (red) cells were subcutaneously injected in mice (1 side) and irradiated for *UROS* KO 3 times per week for 5 weeks at 530 nm. Illumination is indicated by purple light. Five mice per group. (B) Volume of tumor over time. Crosses mean that all of the mice in a group are dead. Mean ± SEM. (C) Kaplan-Meier plot for survival of mice with PC3 tumors treated or not by LV-*UROS*-Cas9 and repeated long-term 530-nm light. Statistical difference by Mantel-Cox test.

molecular status of relapsing tumor cells by PCR. Sanger analysis revealed the persistence of a high proportion of *UROS* KO cells in illuminated tumors (Figure S3). Therefore, at sacrifice, edited cells were still present. Histological analysis of tumors at sacrifice reveals a high modification of tumor structures (Figure S4). After long-term light, tumors are disorganized and pauci-cellular. Importantly, we observed a large peripheral reactional fibrosis. It suggests that regular external percutaneous long-term illumination did not reach the tumor cells, which could explain the relapse. Even though the tumors could not be completely eradicated, 530-nm light exposure of *UROS* KO PC3 tumors dramatically increased survival compared to control groups without gene therapy and *UROS* KO PC3 cells without light. Survival was increased 3-fold (42 versus 14 days in the other conditions; Figure 5C).

## DISCUSSION

We demonstrate that a CRISPR-Cas9-based gene therapy for *UROS* inactivation induces a high accumulation of porphyrins. As in CEP, these metabolic compounds are highly photosensitive. Lighting at 530 nm combined with gene therapy led to the death of cancer cells *in vitro* without any side effect (i.e., no mortality in nontransduced cells). Remarkably, we obtained *in vivo* tumor regression associated with a major increase in mice survival.

Owing to its high penetrance in tissues, a 630-nm wavelength is often used for photodynamic therapy (PDT). However, it may prove nonoptimal with only partial *in vitro* efficacy.[15–19] The 405-nm wavelength, which is the Soret band of porphyrins (optimal absorbance), was highly efficient but induced dermatoxicity and had very low tissue penetrance. As a compromise, we used a 530-nm wavelength to avoid skin damage while maintaining medium penetrance and high *in vitro* efficacy. Using external illumination of the subcu-

taneous engrafted tumors (with the presence of the skin between light and the tumor), we obtained a satisfactory tumor response with tumor regression. Although these results obtained with an external light-emitting diode (LED) are promising, a therapeutic escape occurred. This may have been caused by a reduction in illumination penetrance due to the remodeling of tumoral and peritumoral tissues. Thanks to the advent of interstitial lasers, it is now possible with endoscopic optical fibers to illuminate the interior of tumors, in direct contact with cancer cells.[20,21] Therefore, interstitial illumination combined with *UROS* gene therapy may lead to a longer response to treatment and could overcome the relapse. Moreover, human cancer cell xenografts require immunodeficient mice. We hypothesize that immunocompetent models obtained by using syngeneic mouse prostate tumors should allow the recruitment of the immune system, thus reinforcing the efficacy of our approach. Indeed, PDT is closely associated with strong immunogenic cell death through the emission of damage-associated molecular patterns that attract and activate different immune cells.[22]

Our approach is an alternative to PDT, which uses an exogenous systemic photosensitizer (PS) drug such as aminolevulinic acid (ALA) to accumulate type IX protoporphyrins (PpIX) or light-activated vascular occluding agents such as TOOKAD.[23] The two main limitations of PDT are an obstacle to its use in clinical practice for treating severe cancers and metastasis: (1) the low tumor specificity of PS accumulation in all tissues, and (2) the low intratumoral concentration of PS in cancer cells after systemic administration of exogenous PS. ALA-PDT as a monotherapy often fails to achieve satisfactory clinical outcomes for treating cancer patients. Accumulated PpIX concentrations are low in tumors,[24,25] and they induce the overexpression of inducible nitric oxide (NO) synthase and NO,[26,27] resulting in a high rate of incomplete treatment response and disease relapse. Thanks to *UROS* gene therapy, we obtained high porphyrin concentrations in cancer cells without direct toxicity—in other words, without light, which is essential for preventing treatment side effects and toxicity. Moreover, the type of porphyrin is different. The UROS deficit in CEP induces type I

porphyrin accumulation and severe mutilating skin lesions exposed to sunlight, compared to the ferrochelatase deficit in erythropoietic protoporphyria, which leads to type IX protoporphyrins associated with benign skin redness. These clinical data suggest that *UROS*-edited cells accumulating cytosolic type I porphyrins are more photocytotoxic than mitochondrial type IX protoporphyrin and could be an attractive alternative to conventional PDT.

This preclinical proof of concept was achieved by using prostate cancer cells, since the prostate seems to be a relevant site for cancer gene therapy. It is accessible for the direct injection of intratumoral gene therapy and can be treated by illumination with optical fibers through endoscopes. Prostate cancer illumination has already been used in Phase III/IV of the PDT clinical trial NCT01310894 (this trial has been registered at ClinicalTrials.gov). They combined a systemic intravenous injection of padeliporfin to a multiple insertion of optical fibers in the prostate.[28] Several gene therapy clinical trials have already been approved for prostate cancer. Intratumoral injection is already a therapeutic option, for example, in cancer immunotherapy. Intratumoral delivery provides a promising strategy for harnessing the power of immunotherapy while minimizing off-target toxicities. A needle guided by magnetic resonance imaging ultrasound fusion technology into the prostate gland can be used to inject antibodies, cytokines, or oncolytic viruses.[29] Most of them target the tumor microenvironment and immune response. They include vaccine-based strategies,[30,31] and alteration of the immune microenvironment by interleukin-2[32] and CAR-T cells.[33,34] Protocols directly targeting prostate cancer cells are still rare and include suicide gene,[35–38] oncolytic vectors,[39] suppressor gene activation (p53),[40] GLIPR1,[41] DDX5 mRNA targeting,[42] and vascular-targeted PDT.[28] Despite some preclinical success, gene therapy is not yet routinely used for treating prostate cancer. Our strategy, mimicking a genetic disease to weaken the cancer cells combined with local tumor illumination, is a novel approach and could be a promising alternative. It allows a high specificity and efficacy in the lighted area without any peritumoral toxicity.

In this study, we *ex vivo* inactivated *UROS* before subcutaneous grafting as a proof of concept. In the future, the efficacy and safety of the approach should be tested after orthotopic prostatic grafting.[43] The *in vivo* injection of intraprostatic CRISPR-gene therapy viral and virus-like particle vectors or electroporation of ribonucleoprotein/mRNA should allow specific porphyrin accumulation in the targeted organ. This is an attractive approach because the CRISPR vehicles, injected directly into the tumor, will be concentrated in a restricted area limiting side effects. As already described for retrovirus, there is a theoretical risk of integration of the provirus near an oncogene (insertional mutagenesis). However, in cancer treatment, most of the transduced cells will be eliminated. Cas9 expression can also be immunogenic.[44] For cancer treatment, it would be an advantage to recruit immune cells. Intratumoral injection of lentiviruses is an attractive way to modulate UROS in cancer cells because lentiviruses will not be degraded by the human complement[45] and have high transduction efficacy. Publications already reported their efficiency in reducing tumor volumes after intratumoral injection in murine models.[46,47] Unlike PS accumulation, the transgenic expression of CRISPR-Cas9 can be restricted to cancer cells under the control of a prostatic cancer promoter such as DD3/PCA3.[48,49] Importantly, lentiviruses can also be pseudotyped with more specific envelope glycoprotein to specifically target cancer cells. For example, we published that Sindbis glycoprotein with MUC4 antibody can recognize and target pancreatic cancer cells.[50] Similarly, it would be possible to use targeted vehicles with anti-PSMA, which is highly expressed on the surface of prostate cancer cells.[51,52] Nevertheless, type I porphyrin accumulation alone is not directly toxic for cells and its combination with illumination is mandatory so as to be efficient. This is illustrated in CEP patients whose internal organs are not altered by porphyrin accumulation. By combining a local production of endogenous prostatic porphyrin with a local illumination, we propose a very novel and safe approach. Even if gene therapy is not restricted to cancer cells, only the illuminated cells will die, thereby allowing temporal and spatial specificity. Together, the present findings show that CRISPR-Cas9 offers new insights into cancer gene therapy to inactivate the canonical metabolic pathway essential to cancer cell survival. Knowledge of the hereditary metabolic diseases would likely lead to new anticancer approaches.

## MATERIALS AND METHODS

### Cell culture

The PC3 cell line was a gift from the Mariangela Figini lab.[53] This cell line is modified and stably expresses PSMA, as developed by W.D.W. Heston and colleagues.[54] Cells were maintained *in vitro* at 37°C in a humidified atmosphere of 5% $CO_2$/95% air in RPMI 1640, glutaMAX (Gibco, Thermo Fisher Scientific, Carlsbad, CA), 10% fetal bovine serum, and 1% penicillin-streptomycin (Eurobio Scientific, Les Ulys, France). Cell lines were maintained mycoplasma-free through monthly testing by PCR. For *in vivo* bioluminescence monitoring, cells (PSMA$^+$ PC3 PIP [PC3] and *UROS* KO PSMA+PC3 PIP [*UROS* KO PC3]) were stably transfected using lipofectamine (Invitrogen, Carlsbad, CA) with a plasmid coding for luciferase under the control of cytomegalovirus (CMV) promoter (pcDNA6.2-CMV),[55] and selected by blasticidin (10 μg/mL, Euromedex, Souffelweyersheim, France).

### Lentivector construction and production

Lentivirus vector was produced by the Vect'UB service platform (INSERM US 005–CNRS UMS 3427-TBM-Core, Université de Bordeaux, Bordeaux, France). We designed a lentiviral vector (called LV-*UROS*-Cas9) containing a gRNA against exon 4 *UROS* (GGAA GCAGCAGAGTTATGTT) under the control of the U6 promoter, CRISPR-Cas9 nuclease DNA under the control of the EF1-α promoter, and the Zs-Green reporter to control transduction efficiency. LentiCRISPR version 2 (Zhang lab) was modified to replace the PuroR gene with the Zs-Green gene. LentiCRISPR version 2 was a gift from Feng Zhang (Addgene plasmid no. 52961; https://www.addgene.org/52961; RRID: Addgene_52961). Synthetic gRNA oligonucleotides were cloned into pLentiCRISPR-Zs-Green-modified vector at BsmBI restriction sites.

### UROS gene editing in PC3 cells and tumors

For the *in vitro* study, we transduced PC3 cells with LV-UROS-Cas9 particles (MOI 20). We monitored cell transduction efficiency by cytometry using Zs-Green reporter expression. To validate CRISPR double-stranded break efficiency in PC3 cells and the presence of indels in the *UROS* gene, genomic DNA of transduced PC3 cells was extracted using Nucleospin Tissue (Macherey-Nagel, Düren, Germany) according to the manufacturer's protocol. The genomic region flanking the expected cut site was amplified by PCR (HotStarTaq Plus DNA polymerase, Qiagen, Venlo, the Netherlands) with human primers *UROS* F TAGTTCCAGGCACATAGTAAGCAC and *UROS* R AGGAGGTG AACAACGAATAGACAG. PCR products were purified with Nucleospin Gel and PCR Clean-up (Macherey-Nagel). To check the presence of *UROS* KO cells in tumors with or without illumination, gDNA of tumors was extracted with the Maxwell RSC DNA FFPE Kit (Promega, Charbonnières-les-Bains, France). Extracted DNA was eluted in 70 μL nuclease-free water, and the DNA concentration was determined by fluorimetry with the DS11FX automated system (DeNovix, Wilmington, DE). The genomic region flanking the expected cut site was amplified by PCR (HotStarTaq Plus DNA polymerase, Qiagen) with human primers *UROS* F GGTGTGCAGCTTTCTCATCC and *UROS* R AAACTGAAGGTGAGGGTGGG. PCR products were purified with Nucleospin Gel and PCR Clean-up (Macherey-Nagel). Sanger sequencing was done on purified PCR products and sequenced by LIGHTRUN (GATC Biotech, Konstanz, Germany). Sanger sequencing data were analyzed using ICE version 2 CRISPR Analysis tool software (Synthego, Redwood City, CA). Purified PCR products from nonedited cells were used as the control chromatogram.

### Porphyrin accumulation in PC3 cells

Porphyrins are red fluorescent compounds. Intracellular total porphyrin contents were determined after extraction with methanol/perchloric acid 1 M (30/70 v/v) and quantified by spectrofluorimetry (Hitachi F-4500 fluorescence spectrophotometer) using commercially available calibrators (ClinCal Urine Calibrator Recipe). Cells were also analyzed at 550-nm emission wavelength with a 405-nm excitation laser on a fluorescence-activated cell sorting (FACS) flow cytometer (Per-CP channel, BD Biosciences Accuri C6 Plus apparatus), and the data were analyzed with BD CSampler software (BD Biosciences, Le Pont de Claix, France).

### *In vitro* illumination of PC3 cells

PSMA[+] PC3 PIP cells were plated at $10^5$ cells/well in a 48-well plate and incubated overnight. The next day, the cells were either irradiated, without cover, by a system with interchangeable LED light sources (Thorlabs, wavelengths 405, 530, or 660 nm) or were not irradiated. To control the light source, we monitored light fluence by a light meter (Thorlabs, Newton, NJ), and we protected the other wells from light with an opaque mask. Cell viability was measured by cell count 72 h postirradiation.

### Tumor generation and *in vivo* illumination

All of the experimental procedures involving animals were approved by the Institutional Animal Care and Use Committee of Bordeaux University (agreement no. 25312) and complied with the French and European regulations on Animal Welfare and Public Health Service. Immunodeficient male NSG (NOD/SCID/IL-2Rγnull) mice were housed at the Bordeaux University facility and maintained under 12-h dark/light cycles with water and food provided *ad libitum*. Human PC3 cells ($2 \times 10^6$/100 μL) were implanted subcutaneously in 10-week-old NSG mice on the top of the back (flanks). One week after cell injection, when the tumor diameter had reached 3–5 mm, mice were shaved with clippers and treated with illumination with the same system as for *in vitro* illumination. For irradiation, the mouse was placed on a thermostatically controlled bed, and its skin was protected from light by an opaque mask that had a 10-mm hole to allow the tumor to be irradiated. The light source was positioned 4 cm from the skin and irradiation was performed for 20 min (Figure S3)

### Antitumor efficacy in subcutaneous xenograft model

Tumor progression was monitored either by measuring subcutaneous tumor volume using the formula [volume = $\pi/6.f.(length.width)^{3/2}$] mm3, f = 1.69 for male],[56] using a caliper, or by *in vivo* BLI at the Vivoptic platform (University of Bordeaux, CNRS, INSERM, TBM-Core, Bordeaux, France). BLI was performed using the Lumina LT Imaging system (PerkinElmer, Boston, MA). D-Luciferin (Promega, 2.9 mg/100 μL PBS) was injected intraperitoneally, and bioluminescence acquisition (1 min 4 × 4 binning) and photographs (100 ms) were taken 8 min after substrate injection. Data were analyzed with Living Image software (PerkinElmer). After sacrifice, tumor weight was evaluated using a Sartorius balance. Mice were euthanized and scored as death if tumor diameter was >10 mm or if mice lost more than 10% of their body weight or had signs of discomfort, such as hunched posture, anorexia, or dehydration. For both animal models, the probability of survival was plotted by Kaplan-Meier curves using GraphPad Prism software (GraphPad Software, La Jolla, CA). Tumors were fixed in 10% neutral buffered formalin and embedded in paraffin.

### Statistical analysis

Statistical significance was inferred when necessary. Exact distinct and independent sample size is indicated in each legend (n). GraphPad Prism 6 software was used for the statistical analysis. Results are presented as mean ± SD for *in vitro* experiments and mean ± SEM for *in vivo* experiments. The parametric t test was used when distribution was Gaussian/normal (Shapiro-Wilk test). The nonparametric Mann-Whitney test (two-sided) was used to compare two groups. One-way ANOVA, complemented with the unprotected Fisher's least-significant difference test, was used to compare more than two groups. Survival analyses were performed using GraphPad Prism version 9. p values were calculated by the log-rank (Mantel-Cox) test and were considered significant if less than 0.05.

## DATA AND CODE AVAILABILITY

Most of the data supporting the findings of this study are available within the article [and/or] its supplementary materials. Detailed data are available on request from the corresponding author.

## AUTHOR CONTRIBUTIONS

J.B., F.C., S.D., A. Bedel, and F.M.-G. designed the study, analyzed the data, and drafted the manuscript. V.G.-D. and A. Bibeyran performed the lentivector cloning and production. J.B. performed the gene editing experiments. J.B. and I.L.-G performed the FACS and *in vitro* illumination experiments. M.L. performed the high-performance liquid chromatography (HPLC) porphyrin assay. I.M. and S.A. performed the tumor analysis. C.G. performed the *in vivo* experiments. S.D., E.R., and J.-M.B. held helpful discussions and revised the manuscript. A. Bedel and F.M.-G. were responsible for the supervision of the study and funding acquisition, as well as final approval of the manuscript. All of the authors edited and approved the final manuscript.

## DECLARATION OF INTERESTS

J.B., C.G., S.D., A. Bedel, and F.M.-G. declared patent application EP23 307 258, filed on December 19, 2023, for "Methods of Treating Cancer Combining UROS invalidation and phototherapy."

## REFERENCES

1. Yahya, E.B., and Alqadhi, A.M. (2021). Recent trends in cancer therapy: A review on the current state of gene delivery. Life Sci. *269*, 119087.

2. Wirth, T., Parker, N., and Ylä-Herttuala, S. (2013). History of gene therapy. Gene *525*, 162–169.

3. Scholler, J., Brady, T.L., Binder-Scholl, G., Hwang, W.T., Plesa, G., Hege, K.M., Vogel, A.N., Kalos, M., Riley, J.L., Deeks, S.G., et al. (2012). Decade-long safety and function of retroviral-modified chimeric antigen receptor T cells. Sci. Transl. Med. *4*, 132ra53.

4. Ren, J., Liu, X., Fang, C., Jiang, S., June, C.H., and Zhao, Y. (2017). Multiplex Genome Editing to Generate Universal CAR T Cells Resistant to PD1 Inhibition. Clin. Cancer Res. *23*, 2255–2266.

5. Cullot, G., Boutin, J., Toutain, J., Prat, F., Pennamen, P., Rooryck, C., Teichmann, M., Rousseau, E., Lamrissi-Garcia, I., Guyonnet-Duperat, V., et al. (2019). CRISPR-Cas9 genome editing induces megabase-scale chromosomal truncations. Nat. Commun. *10*, 1136.

6. Robert-Richard, E., Lalanne, M., Lamrissi-Garcia, I., Guyonnet-Duperat, V., Richard, E., Pitard, V., Mazurier, F., Moreau-Gaudry, F., Ged, C., and de Verneuil, H. (2010). Modeling of congenital erythropoietic porphyria by RNA interference: a new tool for preclinical gene therapy evaluation. J. Gene Med. *12*, 637–646.

7. Ged, C., Mendez, M., Robert, E., Lalanne, M., Lamrissi-Garcia, I., Costet, P., Daniel, J.Y., Dubus, P., Mazurier, F., Moreau-Gaudry, F., and de Verneuil, H. (2006). A knock-in mouse model of congenital erythropoietic porphyria. Genomics *87*, 84–92.

8. Richard, E., Mendez, M., Mazurier, F., Morel, C., Costet, P., Xia, P., Fontanellas, A., Geronimi, F., Cario-André, M., Taine, L., et al. (2001). Gene therapy of a mouse model of protoporphyria with a self-inactivating erythroid-specific lentiviral vector without preselection. Mol. Ther. *4*, 331–338.

9. Fiorito, V., Chiabrando, D., Petrillo, S., Bertino, F., and Tolosano, E. (2019). The Multifaceted Role of Heme in Cancer. Front. Oncol. *9*, 1540.

10. Heinemann, I.U., Jahn, M., and Jahn, D. (2008). The biochemistry of heme biosynthesis. Arch. Biochem. Biophys. *474*, 238–251.

11. Bissell, D.M., Anderson, K.E., and Bonkovsky, H.L. (2017). N. Engl. J. Med. *377*, 862–872.

12. Erwin, A., Balwani, M., and Desnick, R.J.; Porphyrias Consortium of the NIH-Sponsored Rare Diseases Clinical Research Network (2013). Congenital Erythropoietic Porphyria. In GeneReviews® [Internet], M.P. Adam, G.M. Mirzaa, R.A. Pagon, S.E. Wallace, L.J.H. Bean, K.W. Gripp, and A. Amemiya, eds. (University of Washington, Seattle), pp. 1993–2023.

13. Sung, H., Ferlay, J., Siegel, R.L., Laversanne, M., Soerjomataram, I., Jemal, A., and Bray, F. (2021). Global Cancer Statistics 2020: GLOBOCAN Estimates of Incidence and Mortality Worldwide for 36 Cancers in 185 Countries. CA. Cancer J. Clin. *71*, 209–249.

14. Gregg, J.R., and Thompson, T.C. (2021). Considering the potential for gene-based therapy in prostate cancer. Nat. Rev. Urol. *18*, 170–184.

15. Postiglione, I., Barra, F., Aloj, S.M., and Palumbo, G. (2016). Photodynamic therapy with 5-aminolaevulinic acid and DNA damage: unravelling roles of p53 and ABCG2. Cell Prolif. *49*, 523–538.

16. Nakayama, T., Kobayashi, T., Shimpei, O., Fukuhara, H., Namikawa, T., Inoue, K., Hanazaki, K., Takahashi, K., Nakajima, M., Tanaka, T., and Ogura, S.I. (2019). Photoirradiation after aminolevulinic acid treatment suppresses cancer cell proliferation through the HO-1/p21 pathway. Photodiagnosis Photodyn. Ther. *28*, 10–17.

17. Şueki, F., Ruhi, M.K., and Gülsoy, M. (2019). The effect of curcumin in antitumor photodynamic therapy: In vitro experiments with Caco-2 and PC-3 cancer lines. Photodiagnosis Photodyn. Ther. *27*, 95–99.

18. Fukuhara, H., Inoue, K., Kurabayashi, A., Furihata, M., Fujita, H., Utsumi, K., Sasaki, J., and Shuin, T. (2013). The inhibition of ferrochelatase enhances 5-aminolevulinic acid-based photodynamic action for prostate cancer. Photodiagnosis Photodyn. Ther. *10*, 399–409.

19. Chakrabarti, P., Orihuela, E., Egger, N., Neal, D.E., Jr., Gangula, R., Adesokun, A., and Motamedi, M. (1998). Delta-aminolevulinic acid-mediated photosensitization of prostate cell lines: implication for photodynamic therapy of prostate cancer. Prostate *36*, 211–218.

20. Shafirstein, G., Bellnier, D., Oakley, E., Hamilton, S., Potasek, M., Beeson, K., and Parilov, E. (2017). Interstitial Photodynamic Therapy-A Focused Review. Cancers *9*, 12.

21. Baran, T.M., and Foster, T.H. (2014). Comparison of flat cleaved and cylindrical diffusing fibers as treatment sources for interstitial photodynamic therapy. Med. Phys. *41*, 022701.

22. Alzeibak, R., Mishchenko, T.A., Shilyagina, N.Y., Balalaeva, I.V., Vedunova, M.V., and Krysko, D.V. (2021). Targeting immunogenic cancer cell death by photodynamic therapy: past, present and future. J. Immunother. Cancer *9*, e001926.

23. Azzouzi, A.R., Barret, E., Moore, C.M., Villers, A., Allen, C., Scherz, A., Muir, G., de Wildt, M., Barber, N.J., Lebdai, S., and Emberton, M. (2013). TOOKAD® (2013) Soluble vascular-targeted photodynamic (VTP) therapy: determination of optimal treatment conditions and assessment of effects in patients with localised prostate cancer. BJU Int. *112*, 766–774.

24. Choi, S.H., Kim, K.H., and Song, K.H. (2017). Effect of methyl aminolevulinate photodynamic therapy with and without ablative fractional laser treatment in patients with microinvasive squamous cell carcinoma: a randomized clinical trial. JAMA Dermatol. *153*, 289–295.

25. Jansen, M.H.E., Mosterd, K., Arits, A.H.M.M., Roozeboom, M.H., Sommer, A., Essers, B.A.B., van Pelt, H.P.A., Quaedvlieg, P.J.F., Steijlen, P.M., Nelemans, P.J., and Kelleners-Smeets, N.W.J. (2018). Five-year results of a randomized controlled trial comparing effectiveness of photodynamic therapy, topical imiquimod, and topical 5-fluorouracil in patients with superficial basal cell carcinoma. J. Invest. Dermatol. *138*, 527–533.

26. Fahey, J.M., and Girotti, A.W. (2015). Accelerated migration and invasion of prostate cancer cells after a photodynamic therapy-like challenge: Role of nitric oxide. Nitric Oxide *49*, 47–55.

27. Girotti, A.W., Fahey, J.M., and Korytowski, W. (2016). Multiple Means by Which Nitric Oxide can Antagonize Photodynamic Therapy. Curr. Med. Chem. *23*, 2754–2769.

28. Azzouzi, A.R., Vincendeau, S., Barret, E., Cicco, A., Kleinclauss, F., van der Poel, H.G., Stief, C.G., Rassweiler, J., Salomon, G., Solsona, E., et al. (2017). PCM301 Study Group. Padeliporfin vascular-targeted photodynamic therapy versus active surveillance in men with low-risk prostate cancer (CLIN1001 PCM301): an open-label, phase 3, randomised controlled trial. Lancet Oncol. 18, 181–191.

29. Hong, W.X., Haebe, S., Lee, A.S., Westphalen, C.B., Norton, J.A., Jiang, W., and Levy, R. (2020). Intratumoral Immunotherapy for Early-stage Solid Tumors. Clin. Cancer Res. 26, 3091–3099.

30. McNeel, D.G., Dunphy, E.J., Davies, J.G., Frye, T.P., Johnson, L.E., Staab, M.J., Horvath, D.L., Straus, J., Alberti, D., Marnocha, R., et al. (2009). Safety and immunological efficacy of a DNA vaccine encoding prostatic acid phosphatase in patients with stage D0 prostate cancer. J. Clin. Oncol. 27, 4047–4054.

31. McNeel, D.G., Eickhoff, J.C., Johnson, L.E., Roth, A.R., Perk, T.G., Fong, L., Antonarakis, E.S., Wargowski, E., Jeraj, R., and Liu, G. (2019). Phase II Trial of a DNA Vaccine Encoding Prostatic Acid Phosphatase (pTVG-HP [MVI-816]) in Patients with Progressive, Nonmetastatic, Castration-Sensitive Prostate Cancer. J. Clin. Oncol. 37, 3507–3517.

32. Belldegrun, A., Tso, C.L., Zisman, A., Naitoh, J., Said, J., Pantuck, A.J., Hinkel, A., deKernion, J., and Figlin, R. (2001). Interleukin 2 gene therapy for prostate cancer: phase I clinical trial and basic biology. Hum. Gene Ther. 12, 883–892.

33. Parsons, J.K., Pinto, P.A., Pavlovich, C.P., Uchio, E., Kim, H.L., Nguyen, M.N., Gulley, J.L., Jamieson, C., Hsu, P., Wojtowicz, M., et al. (2018). A Randomized, Double-blind, Phase II Trial of PSA-TRICOM (PROSTVAC) in Patients with Localized Prostate Cancer: The Immunotherapy to Prevent Progression on Active Surveillance Study. Eur. Urol. Focus 4, 636–638.

34. Narayan, V., Barber-Rotenberg, J.S., Jung, I.Y., Lacey, S.F., Rech, A.J., Davis, M.M., Hwang, W.T., Lal, P., Carpenter, E.L., Maude, S.L., et al. (2022). PSMA-targeting TGFβ-insensitive armored CAR T cells in metastatic castration-resistant prostate cancer: a phase 1 trial. Nat. Med. 28, 724–734.

35. Herman, J.R., Adler, H.L., Aguilar-Cordova, E., Rojas-Martinez, A., Woo, S., Timme, T.L., Wheeler, T.M., Thompson, T.C., and Scardino, P.T. (1999). In situ gene therapy for adenocarcinoma of the prostate: a phase I clinical trial. Hum. Gene Ther. 10, 1239–1249.

36. Miles, B.J., Shalev, M., Aguilar-Cordova, E., Timme, T.L., Lee, H.M., Yang, G., Adler, H.L., Kernen, K., Pramudji, C.K., Satoh, T., et al. (2001). Prostate-specific antigen response and systemic T cell activation after in situ gene therapy in prostate cancer patients failing radiotherapy. Hum. Gene Ther. 12, 1955–1967.

37. Peng, W., Anderson, D.G., Bao, Y., Padera, R.F., Jr., Langer, R., and Sawicki, J.A. (2007). Nanoparticulate delivery of suicide DNA to murine prostate and prostate tumors. Prostate 67, 855–862.

38. Hattori, Y., and Maitani, Y. (2005). Folate-linked nanoparticle-mediated suicide gene therapy in human prostate cancer and nasopharyngeal cancer with herpes simplex virus thymidine kinase. Cancer Gene Ther. 12, 796–809.

39. DeWeese, T.L., van der Poel, H., Li, S., Mikhak, B., Drew, R., Goemann, M., Hamper, U., DeJong, R., Detorie, N., Rodriguez, R., et al. (2001). A phase I trial of CV706, a replication-competent, PSA selective oncolytic adenovirus, for the treatment of locally recurrent prostate cancer following radiation therapy. Cancer Res. 61, 7464–7472.

40. Pisters, L.L., Pettaway, C.A., Troncoso, P., McDonnell, T.J., Stephens, L.C., Wood, C.G., Do, K.A., Brisbay, S.M., Wang, X., Hossan, E.A., et al. (2004). Evidence that transfer of functional p53 protein results in increased apoptosis in prostate cancer. Clin. Cancer Res. 10, 2587–2593.

41. Sonpavde, G., Thompson, T.C., Jain, R.K., Ayala, G.E., Kurosaka, S., Edamura, K., Tabata, K.i., Ren, C., Goltsov, A.A., Mims, M.P., et al. (2011). GLIPR1 tumor suppressor gene expressed by adenoviral vector as neoadjuvant intraprostatic injection for localized intermediate or high-risk prostate cancer preceding radical prostatectomy. Clin. Cancer Res. 17, 7174–7182.

42. Le, T.K., Cherif, C., Omabe, K., Paris, C., Lannes, F., Audebert, S., Baudelet, E., Hamimed, M., Barbolosi, D., Finetti, P., et al. (2023). DDX5 mRNA-targeting antisense oligonucleotide as a new promising therapeutic in combating castration-resistant prostate cancer. Mol. Ther. 31, 471–486.

43. Liu, W., Zhu, Y., Ye, L., Zhu, Y., and Wang, Y. (2022). Establishment of an orthotopic prostate cancer xenograft mouse model using microscope-guided orthotopic injection of LNCaP cells into the dorsal lobe of the mouse prostate. BMC Cancer 22, 173.

44. Hakim, C.H., Kumar, S.R.P., Pérez-López, D.O., Wasala, N.B., Zhang, D., Yue, Y., Teixeira, J., Pan, X., Zhang, K., Million, E.D., et al. (2021). Cas9-specific immune responses compromise local and systemic AAV CRISPR therapy in multiple dystrophic canine models. Nat. Commun. 12, 6769.

45. Sheridan, P.L., Bodner, M., Lynn, A., Phuong, T.K., DePolo, N.J., de la Vega, D.J., Jr., O'Dea, J., Nguyen, K., McCormack, J.E., Driver, D.A., et al. (2000). Generation of retroviral packaging and producer cell lines for large-scale vector production and clinical application: improved safety and high titer. Mol. Ther. 2, 262–275.

46. Wu, V.J., Pang, D., Tang, W.W., Zhang, X., Li, L., and You, Z. (2017). Obesity, age, ethnicity, and clinical features of prostate cancer patients. Am. J. Clin. Exp. Urol. 5, 1–9.

47. Park, J.H., Seo, J.H., Jeon, H.Y., Seo, S.M., Lee, H.K., Park, J.I., Kim, J.Y., and Choi, Y.K. (2020). Lentivirus-Mediated VEGF Knockdown Suppresses Gastric Cancer Cell Proliferation and Tumor Growth in vitro and in vivo. OncoTargets Ther. 13, 1331–1341.

48. Verhaegh, G.W., van Bokhoven, A., Smit, F., Schalken, J.A., and Bussemakers, M.J. (2000). Isolation and characterization of the promoter of the human prostate cancer-specific DD3 gene. J. Biol. Chem. 275, 37496–37503.

49. Salameh, A., Lee, A.K., Cardó-Vila, M., Nunes, D.N., Efstathiou, E., Staquicini, F.I., Dobroff, A.S., Marchiò, S., Navone, N.M., Hosoya, H., et al. (2015). PRUNE2 is a human prostate cancer suppressor regulated by the intronic long noncoding RNA PCA3. Proc. Natl. Acad. Sci. USA 112, 8403–8408.

50. Lafitte, M., Rousseau, B., Moranvillier, I., Taillepierre, M., Peuchant, E., Guyonnet-Dupérat, V., Bedel, A., Dubus, P., de Verneuil, H., Moreau-Gaudry, F., and Dabernat, S. (2012). In vivo gene transfer targeting in pancreatic adenocarcinoma with cell surface antigens. Mol. Cancer 11, 81.

51. Nauseef, J.T., Bander, N.H., and Tagawa, S.T. (2021). Emerging prostate-specific membrane antigen-based therapeutics: small molecules, antibodies, and beyond. Eur. Urol. Focus 7, 254–257.

52. Yadav, M.P., Ballal, S., Sahoo, R.K., Dwivedi, S.N., and Bal, C. (2019). Radioligand Therapy With 177Lu-PSMA for Metastatic Castration-Resistant Prostate Cancer: A Systematic Review and Meta-Analysis. AJR Am. J. Roentgenol. 213, 275–285.

53. Frigerio, B., Franssen, G., Luison, E., Satta, A., Seregni, E., Colombatti, M., Fracasso, G., Valdagni, R., Mezzanzanica, D., Boerman, O., et al. (2017). Full preclinical validation of the 123I-labeled anti-PSMA antibody fragment ScFvD2B for prostate cancer imaging. Oncotarget 8, 10919–10930.

54. Ghosh, A., Wang, X., Klein, E., and Heston, W.D.W. (2005). Novel role of prostate-specific membrane antigen in suppressing prostate cancer invasiveness. Cancer Res. 65, 727–731.

55. Mazzocco, C., Fracasso, G., Germain-Genevois, C., Dugot-Senant, N., Figini, M., Colombatti, M., Grenier, N., and Couillaud, F. (2016). In vivo imaging of prostate cancer using an anti-PSMA scFv fragment as a probe. Sci. Rep. 6, 23314.

56. Feldman, J.P., Goldwasser, R., Mark, S., Schwartz, J., and Orion, I. (2009). A Mathematical model for tumour volume evaluation using two dimensions. J.Appl Quant Methods. 4, 455–462.